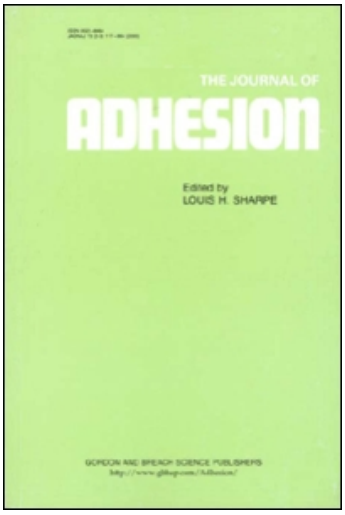

The Journal of Adhesion
Publication details, including instructions for authors and subscription information:
http://www.informaworld.com/smpp/title~content=t713453635

Adhesion and Failure Mechanisms of a Model Hot Melt Adhesive Bonded to Polypropylene

M. F. Tse[a]; G. R. Hamed[b]; A. Tathgur[b]
[a] Polymer Science Division, Baytown Polymers Center, Exxon Chemical Company, Baytown, Texas, USA [b] Department of Polymer Science, University of Akron, Akron, Ohio, USA

To cite this Article Tse, M. F. , Hamed, G. R. and Tathgur, A.(1997) 'Adhesion and Failure Mechanisms of a Model Hot Melt Adhesive Bonded to Polypropylene', The Journal of Adhesion, 61: 1, 1 — 25
To link to this Article: DOI: 10.1080/00218469708010513
URL: http://dx.doi.org/10.1080/00218469708010513

J. Adhesion, 1997, Vol. 61, pp. 1–25
Reprints available directly from the publisher
Photocopying permitted by license only

Adhesion and Failure Mechanisms of a Model Hot Melt Adhesive Bonded to Polypropylene*

M. F. TSE[a], G. R. HAMED[b] and A. TATHGUR[b]

[a]*Polymer Science Division, Baytown Polymers Center, Exxon Chemical Company, Baytown, Texas 77522, USA;*
[b]*Department of Polymer Science, University of Akron, Akron, Ohio 44325, USA*

(Received 25 August 1995; In final form 9 April 1996)

A model hot melt adhesive (HMA) based on an ethylene/vinyl acetate copolymer (EVA), an Escorez® hydrocarbon tackifier, and a wax has been used to bond together polypropylene (PP) films to give equilibrium bonding. Peel strengths were determined over a broad range of peel rates and test temperatures. Contrary to the peel behavior of joints with simple rubbery adhesives [1], peel strengths with this semi-crystalline adhesive are not rate-temperature superposable, and multiple transitions in failure locus occur. The semi-crystalline structure of the HMA also prevents rate-temperature superposition of its dynamic moduli.

At different test temperatures, the dependence of peel strength on peel rate shows some resemblance to the dependence of the loss tangent of the bulk adhesive on frequency. This is consistent with a previous result [2] that the HMA debonding term, D, varies with the loss tangent of a HMA at the T-peel debonding frequency.

This model HMA, similar to block copolymer/tackifier blends [3], consists of two phases: an EVA-rich and a tackifier-rich phase, in its amorphous region. At a low peel rate of 8.33×10^{-5} m/s, the peel strength shows a maximum at a temperature that corresponds to the transition temperature of the tackifier-rich phase (T_1'). At a higher peel rate of 8.33×10^{-3} m/s, the peel strength rises with increasing test temperature, but becomes essentially constant at temperature T_1'. It is believed that, to optimize the peel strength of a HMA at ambient temperature, it is advantageous to formulate the EVA polymer (or other semi-crystalline polyolefins) with a compatible tackifier that yields a tackifier-rich phase with a transition temperature (T_1') in the vicinity of room temperature.

Keywords: Hot melt adhesive; tackifier; polypropylene; adhesion; failure mechanism; peel strength; rate-temperature superposition; storage modulus; loss modulus; loss tangent; debonding frequency

*Previously presented at the Second European Industrial Adhesives Conference, Brussels, Belgium, April 27, 1995.

INTRODUCTION

The main purpose of this work is to provide a better understanding of how the peel strength and failure mode of a model adhesive of a semi-crystalline polymer vary with peel rate and test temperature, and to test the applicability of the time-temperature superposition principle [4] to this adhesive system. Also, it is desired to correlate peel adhesion with the phase structure of the adhesive.

Strength of Adhesives and Joints

The strength of an adhesive joint is best quantified by measuring the fracture energy, G_a, which is the energy required to cause a unit area of failure. It is customary to give the fracture energy a subscript indicative of the fracture locus. For examples, G_{ai} denotes interfacial failure (I), whereas G_{ac} denotes cohesive failure (C). Perhaps the simplest geometry for measuring G_a is the peeling geometry. In this test, unlike *e.g.*, the butt tensile or lap shear tests, G_a is given directly by the fracturing force. In addition, fracture progresses at a relatively constant rate. One peel test method in which two strips of an adhesive joint are peeled apart symmetrically in opposite directions is denoted "T-peeling". If the separated substrates are not elongated significantly, then

$$G_a = 2F/w = 2P \tag{1}$$

where F is the peel force, w is the width of the bonded strips, and P is defined as the peel strength.

Viscoelastic Effects in Adhesion

Standardized industrial peel testing is normally done at a single test rate and temperature. However, an adhesive joint, when in service, may be exposed to different deformation rates and temperatures. Therefore, peel strengths at various rates/temperatures are necessary to understand joint performance in real service.

As test rate and temperature vary, the strength of an adhesive joint changes. With amorphous, elastomeric adhesives, joint strengths usually

increase with increasing rate or decreasing temperature. Furthermore, failure modes change with test conditions [1]. Many adhesive joints exhibit a cohesive failure mode within the adhesive at low rates or high temperatures, but show interfacial failure when tested at high speeds or low temperatures. Of course, these phenomena are the result of the viscoelastic nature of the adhesive [5], as discussed further below.

Figure 1 shows the peel strength of an SBR elastomer model adhesive adhering to Mylar® [1]. At low peel rates, the peel force increases with rate and the joint fails cohesively (C) as the adhesive flows apart. Beyond a critical peel rate, the peel force drops abruptly and the joint fails interfacially (I). This critical peel rate depends upon test temperature. It is necessary to peel faster to cause the C-to-I transition at a higher test temperature. The C-to-I transition can be explained as follows. At sufficiently low peel rates, the adhesive molecules are able to disentangle and flow apart like a liquid. Although the local stress required to disentangle adhesive molecules at low rates is relatively low, the work of extending a viscoelastic liquid (ductile flow) to the point of rupture is large. Above the critical rate, the adhesive molecules remain intertwined as a coherent elastic solid. Molecules are unable to disentangle

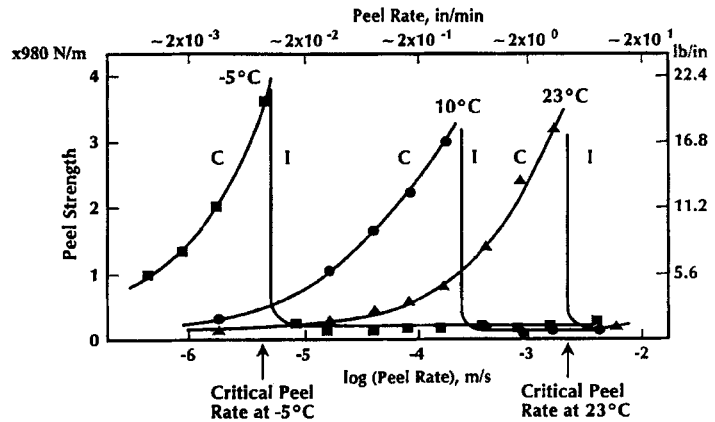

- For A Given Temperature, Transition Of Cohesive (C) To Interfacial (I) Failure Mode Occurs At A Critical Peel Rate, R_c
- R_c Increases With Increasing Temperature

FIGURE 1 Peel strengths of a model SBR adhesive bonded to Mylar® depend on rate and temperature; 1 lb/in = 175 N/m and 1 in/min = 4.25×10^{-4} m/s. (After Ref. 1).

and flow because the rate of deformation of the adhesive layer at the peel front is high. In this elastic or rubbery state, the peel force depends more strongly upon interfacial attractions, and is relatively small.

The force-rate curves at different temperatures can be superimposed to give a single master curve by a horizontal shift along the rate scale (Fig. 2). Provided the adhesive is a simple viscoelastic substance (no crystallinity or phase separation), this shift factor, a_T, takes the universal form described by the WLF equation [4]:

$$\log a_T = -17.4(T - T_g)/[51.6 + (T - T_g)]$$

where a_T = ratio of corresponding test rates at temperatures T and T_g. Moreover, a_T also represents the ratio of the rates of Brownian motion of polymer segments at T and T_g. This master curve has a high peak at low rates where the C-to-I transition occurs. It also has a low

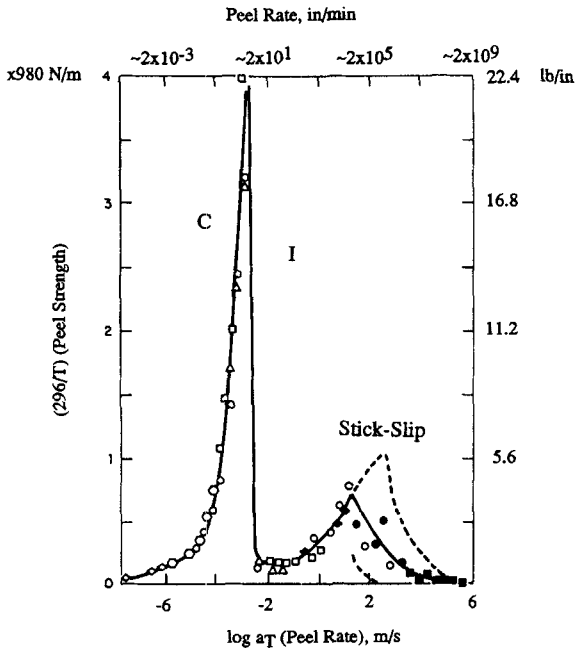

FIGURE 2 Peel strength *versus* peel rate curves of the model SBR adhesive/Mylar® joint at different temperatures are superimposed to a master curve (reference temperature = 10°C) by a horizontal shift along the rate scale. (After Ref. 1).

peak at high rates, where joint failure is interfacial. The dashed lines in this region represent the upper and lower bounds of stick-slip peeling. The success of simple WLF rate-temperature superposition indicates that peel strength is controlled by the segmental mobility of the adhesive. Gent and Petrich [1] also demonstrated that the peak at low rates is associated with a transition from liquid-like to rubber-like behavior, whereas the peak at high rates corresponds to a transition from rubber-like to glass-like behavior.

The universal WLF equation is only applicable to simple viscoelastic substances. However, it recently has been shown that the mechanical response (elastic modulus and fracture energy) of some epoxy and rubber–toughened epoxy adhesives as a function of test rate and temperature can be shifted to form single master curves [6]. Also, the dynamic moduli of low styrene content styrene-isoprene triblock copolymers containing a compatible tackifier can be superimposed over a wide range of frequencies and temperatures [3]. Of course, in these cases, the shift factor a_T is not of universal form; it must be determined experimentally for each adhesive type.

EXPERIMENTAL

Materials and HMA Blending

The EVA polymer (Escorene® 7750; Exxon Chemical), the tackifier (Escorez 2393; Exxon Chemical), the wax (Aristowax® 165; Unocal), and the PP substrate (Escorene® 4252; Exxon Chemical) have been described earlier [2]. The EVA polymer has a vinyl acetate content of 28 wt.%, and a melt index of 32. Escorez 2393 was cationic polymerized from mixed aliphatic and aromatic monomer feeds obtained from petroleum sources. It has a DSC T_g of 45°C. ^{13}C NMR measurements indicated that Aristowax 165 is a linear alkane containing no detectable amount of unsaturation and isolated short chain branching. Therefore, it should have a structure very similar to a low molecular weight polyethylene. The polypropylene contains antioxidant(s) and calcium stearate, but has no slip, anti-block or anti-static agent. Irganox® 1010 (M.P. = 93°C; Ciba-Geigy) was the antioxidant.

Table I shows the model HMA formulations used in this study:

TABLE I Model HMA Formulations

	EVA/Escorez 2393	*EVA/Escorez 2393/Wax*
Escorene 7750	50	45
Escorez 2393	50	45
Aristowax 165	–	10
Iraganox 1010	0.5	0.5

where the numbers under the HMA formulations are expressed in parts by weight. These formulations were blended by taking the EVA and antioxidant in a glass reaction vessel, which was equipped with a mechanical stirrer and heated using a heating mantle. The temperature was maintained at 120°C and nitrogen was purged to create an inert atmosphere. Mixing continued for 5 minutes. Then, the tackifier was added and mixing allowed for 2 additional minutes. At this point, for the EVA/Escorez 2393/Wax HMA, the wax was added and mixing continued for 13 minutes. Total mixing time was 20 minutes. While the mixture was hot, it was poured onto Teflon®-coated aluminum foil in a tray to give a thick sheet of adhesive.

GPC Measurements

Molecular weights of the EVA polymer, the wax and the polypropylene substrate were measured by a Waters GPC 150°C instrument equipped with a four-column, ultra-styragel set with porosities of 10^3, 10^4, 10^5 and 10^6 Å, operated at 145°C. The mobile phase was 1,2,4-trichlorobenzene. The columns were calibrated over the molecular weight range of 5,000–350,000 using narrow molecular weight distributed linear polyethylene standards from NIST (National Institute of Standards and Testing).

The molecular weight determination of the tackifier was performed by using a Waters 410 GPC instrument haivng a five-column set with porosity ranging from 10^2 to 10^5 Å, operated at 30°C. The mobile phase was THF. Column calibrations were obtained with the use of polystyrene standards.

Viscoelastic and Modulated DSC Measurements

A bending mode was used in a Rheometric Scientific DMTA to measure tensile storage moduli, E', tensile loss moduli, E'', and loss tangents, tan δ. Specimens for all viscoelastic studies were made by compression-molding the adhesive material to 1.6 mm thick at 120°C for 5 minutes under 5,000 kg force. Sample sheets were cut into 5 mm wide strips for DMTA measurements. Samples were scanned from -50 to 50°C at an increasing rate of 2°C/min and a frequency of 1 Hz. For frequency-scan experiments, samples were scanned at different frequencies (0.1, 0.3, 1, 3, 5, 10 and 20 Hz) after being held at a given temperature for 3 minutes. Test temperatures were -30, -20, -10, 0, 10, 20, 30, 40, 50 and 60°C.

Also, shear storage moduli, G', shear loss moduli, G'', and loss tangents, tan δ, were measured from -60 to 85°C using a Rheometric Scientific RDS-7700 dynamic spectrometer. Isochronal runs at 10 rad/s were performed using the 8 mm parallel-plate geometry (conditions: strains of 0.1 and 2% for low and high temperature ranges, respectively). The heating rate was estimated to be about 1°C/min.

Thermal response was measured in a modulated DSC (DSC 2910, TA Instruments, Inc., New Castle, DE, USA). An encapsulated sample was first heated at 20°C/min to 150°C, and was held at this temperature for 2 minutes. It was then cooled at 10°C/min to -100°C, and was held at this temperature for 5 minutes. The thermogram was recorded at a heating rate of 5°C/min (modulated at $\pm$ 0.5°C every minute) up to the final temperature of 150°C. The T_g was determined from the mid-point of the thermal transition, whereas the T_m was determined from the endothermic peak, both from the heating cycle. The T_c was determined from the exothermic peak in the cooling cycle.

T-Peel Sample Preparation

Twenty-one grams of adhesive were pressed between two Teflon®-coated aluminum plates using 0.70 mm × 178 mm × 178 mm brass spacers, at 110°C for 5 minutes under 5,000 kg of load. Then, the plates were cooled under tap water, giving a 0.70 mm thick adhesive sheet.

This adhesive sheet and Teflon spacers (0.43 mm thick) were placed between two 0.35 mm × 200 mm × 200 mm PP films. The sandwich was placed between chrome plates, then metal plates, and was pressed at 110°C for 2 hours under a load of 20,000 kg. Contact was prevented at one end by inserting a piece of Mylar® to provide "arms" for subsequent T-peel measurements. For the last 5 minutes, heating was stopped and tap water was used to cool the press. Strips, 25 mm wide, were cut and bond strengths were determined in a T-peel geometry.

Determination of Peel Strength

Specimens were peeled apart at 6 temperatures (0, 10, 20, 35, 40 and 50°C) and 6 rates (8.33×10^{-5}, 1.66×10^{-4}, 8.33×10^{-4}, 1.66×10^{-3}, 3.33×10^{-3}, 8.33×10^{-3} m/s), using an Instron Model 1130 testing machine. The average force required to peel a specimen was determined and the force was then converted to a peel strength by Eq. (1).

RESULTS AND DISCUSSION

Characterization of Various Materials

GPC curves of EVA, Escorez 2393, wax and the PP substrate are shwon in Figure 3, where MW denotes molecular weight. It appears that EVA, wax and PP all have a low molecular weight tail, whereas Escorez 2393 has a high molecular weight tail. Values of M_n, M_w, M_w/M_n and M_z of these materials are shown in Table II.

DSC curves of EVA (cooling and heating cycles) and wax (heating cycle only) are shown in Figure 4. The EVA polymer has a melting temperature, T_m, of 72°C, a crystallization temperature, T_C, of 50°C, and a T_g of −31°C. The wax has a T_m of 68°C.

Phase Structures of HMA

DMTA curves of tan δ *versus* temperature, E'' *versus* temperature and E' *versus* temperature of the two model HMAs (Tab. I) are shown in Figure 5. Similar to block copolymer/tackifier blends [3], two transition

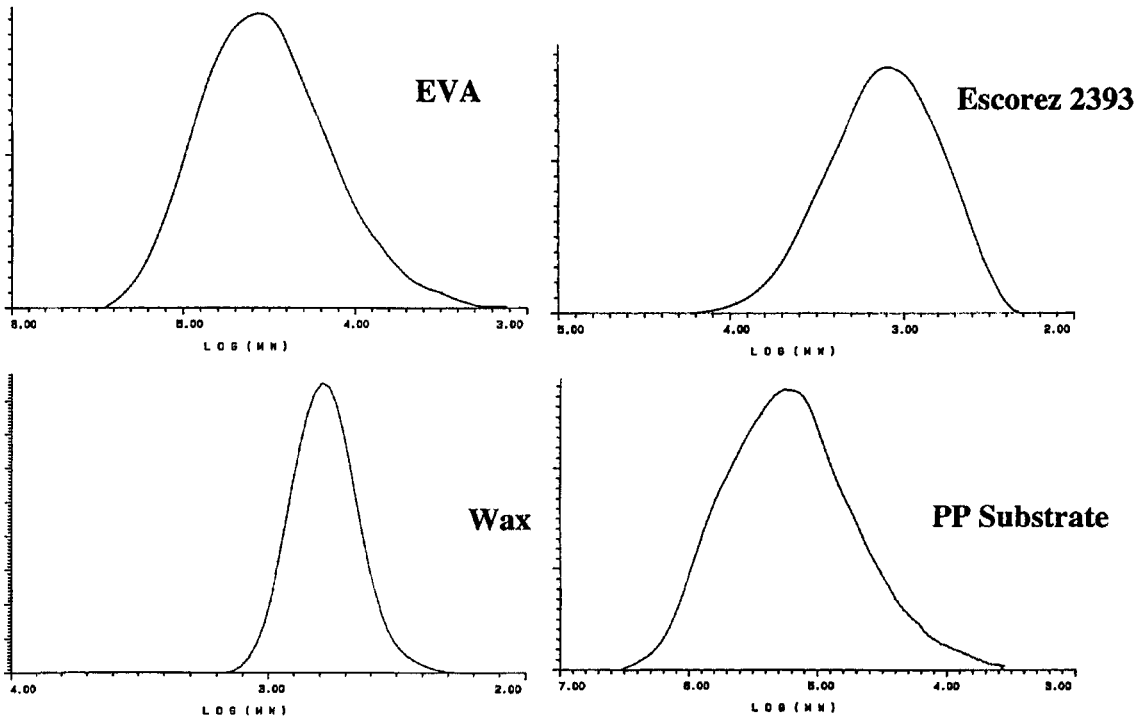

FIGURE 3 GPC curves of EVA, Escorez 2393, wax and polypropylene, where MW denotes the molecular weight and the vertical axis is the differential refractive index.

TABLE II Molecular Weights of EVA, Tackifier, Wax and Substrate

	EVA	*Escorez 2393*	*Wax*	*PP*
M_n	22,000	860	410	80,000
M_w	44,000	1460	460	297,000
M_w/M_n	2.0	1.7	1.1	3.7
M_z	75,000	2700	510	694,000

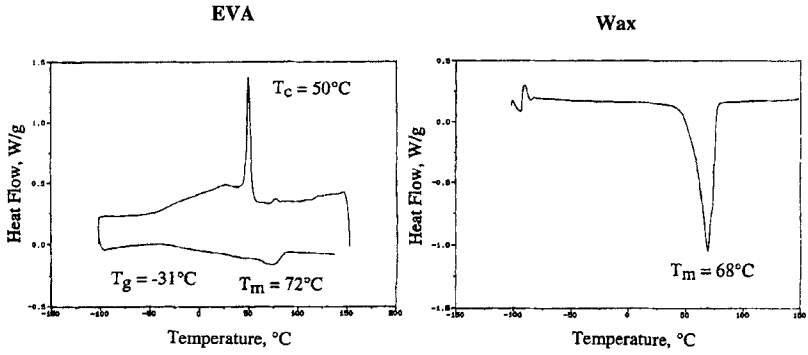

FIGURE 4 DSC thermograms of EVA and wax.

temperatures, $T_{g_1} \sim -8°C$ and $T_1' \sim 35°C$, associated with the EVA-rich phase and the tackifier-rich phase, respectively, are observed. T_{g_1} and T_1' are unambiguously determined from the E'' peak position and the tan δ peak position, respectively. The EVA/Escorez 2393/Wax and the EVA/Escorez 2393 HMAs have similar values of T_{g_1} and T_1', indicating that the wax does not affect these transition temperatures significantly. Moreover, when compared with the EVA/Escorez 2393 HMA, the wax in the EVA/Escorez 2393/Wax HMA increases the peak tan δ of the EVA-rich phase, but decreases the peak tan δ of the tackifier-rich phase. However, wax addition has little effects on E' and E'' at low temperatures, but it enhances these two quantities appreciably at high temperatures.

These T_{g_1} and T_1' transitions in the EVA/Escorez 2393/Wax HMA are further characterized *via* the modulated DSC (Fig. 6). T_{g_1} and T_1' are -21 and 16°C, respectively. Therefore, the blend of EVA (DSC

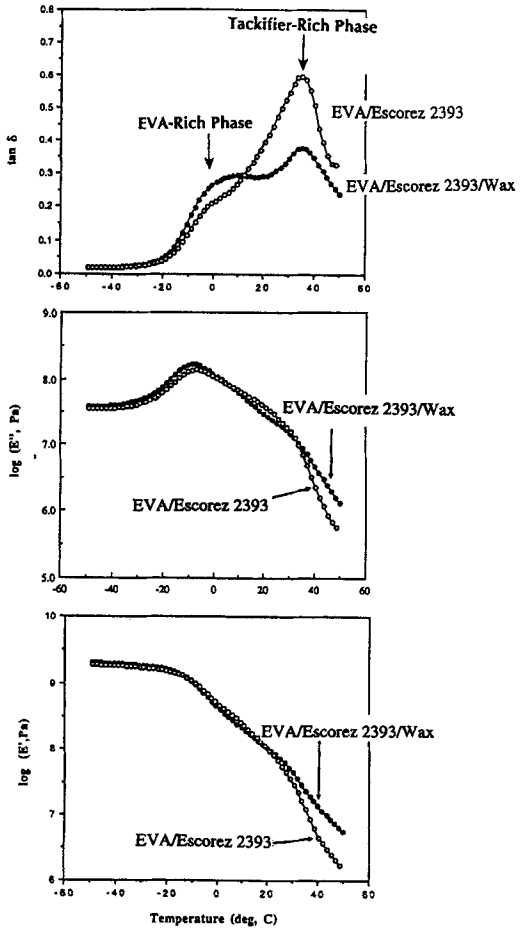

FIGURE 5 DMTA loss modulus and loss tangent curves reveal the existence of two phases in the HMA amorphous region (frequency = 1 Hz).

$T_g = -31°C$ according to Fig. 4), Escorez 2393 (DSC $T_g = 45°$) and wax has DSC transition temperatures of -21 and 16°C. There are at least two pieces of data indicating that Escorez 2393 is not miscible with the amorphous region of the EVA polymer. First, a hydrocarbon tackifier, such as Escorez 2393, is non-polar, whereas the amorphous region of EVA is polar because it is enriched with vinyl acetate segments. Secondly, there is quite a big difference in surface tension

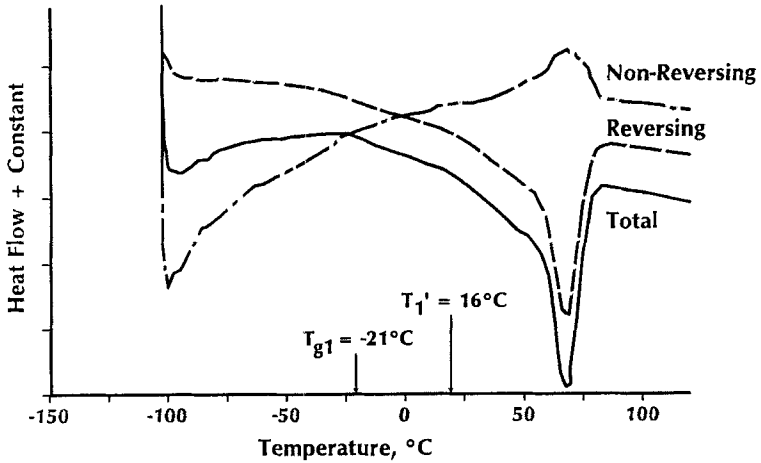

FIGURE 6 Modulated DSC data also reveal the existence of two phases in the HMA amorphous region of the model EVA/Escorez 2393/Wax HMA.

between EVA and Escorez 2393 [2], indicating that they have different thermodynamic behavior. The result is that the blend of EVA/Escorez 2393/Wax has two transition temperature, T_{g_1} and T_1', in between the T_g of EVA and the T_g of Escorez 2393.

The inverted peak at 68°C in Figure 6 represents the HMA melting temperature, T_m. This coincides with the T_m of the wax (Fig. 4). However, it is noted that DSC T_m of the EVA polymer is 72°C (Fig. 4), whereas that of the EVA/Escorez 2393 HMA is 66°C (DSC thermogram not shown). Therefore, the wax appears to raise the T_m of the EVA/Escorez 2393/Wax HMA back up to 68°C.

RDS-7700 curves of tan δ *versus* temperature, G'' *versus* temperature and G' *versus* temperature of the EVA polymer and the EVA/Escorez 2393/Wax model HMA are compared in Figure 7, where G' and G'' are expressed in dynes/cm^2. Similar to DMTA experiments, T_g or T_{g_1} and T_1' are determined from the G'' peak position and the tan δ peak position, respectively. Usually, RDS-7700 measurements yield lower loss modulus and loss tangent peak temperatures than DMTA measurements for the following reason. In a temperature-scan experiment of the RDS-7700, the temperature increases in a 2°C step. Before data acquisition, which takes 1 min, the sample is "thermally-soaked" for 3 min. This amounts to a heating rate of approximately 1°C/min,

which is lower than the 2°C/min in the DMTA temperature scans. For example, loss modulus peak positions from DMTA and RDS-7700 measurements give T_g's of -17°C and -33°C, respectively, for the EVA polymer. Also, Figure 7 indicates that the EVA/Escorez 2393/Wax HMA will begin to melt between 60 and 80°C. This melting transition is well-separated from the T_1' transition of the HMA.

All the above results in Figures 5–7 are summarized in Table III. For the remainder of the discussion for the EVA/Escorez 2393/Wax HMA in this paper, T_{g_1} and T_1' values from the RDS-7700 measurements are primarily empolyed.

Figure 8 shows master curves of E', E'' and tan δ of EVA/Escorez 2393/Wax at a reference temperature of 20°C. Viscoelastic data from the frequency-scan experiments were shifted along the frequency axis. There is no vertical shifting. Due to the semi-crystalline structure of the HMA, rate-temperature superposition appears to fail, especially in the low frequency and/or high temperature regions.

Peel Behavior of HMA

Peel results of the model EVA/Escorez 2393/Wax HMA are detailed in Table IV. A similar peel rate range used by Gent and Petrich [1] was employed. Peel strengths are plotted against peel rate in Figure 9. Two types of behavior are observed. At sub-ambient test temperatures (0–20°C), peel strength decreases as the peel rate increases. The decline is less severe at the lowest temperature, 0°C. However, at test temperatures above ambient temperature (35–50°C), the peel strength increases and converges to an apparent plateau as peel rate increases. The 35, 40 and 50°C curves almost coincide at the highest peel rate. Therefore, this peel behavior for a semi-crystalline adhesive of the EVA polymer is very different from that of the amorphous adhesive of SBR shown in Figure 1.

From the data in Figure 9, the logarithm of peel strength is plotted against temperature at three different rates: 8.33×10^{-5} m/s, 8.33×10^{-4} m/s and 8.33×10^{-3} m/s in Figure 10. As noted before, at low test temperatures, peel strengths at different peel rates do not vary significantly. As test temperature increases, peel strengths are higher at lower peel rates. If the test temperature is further increased beyond $T_1' = 33$°C, the reverse behavior occurs. In the following discussion,

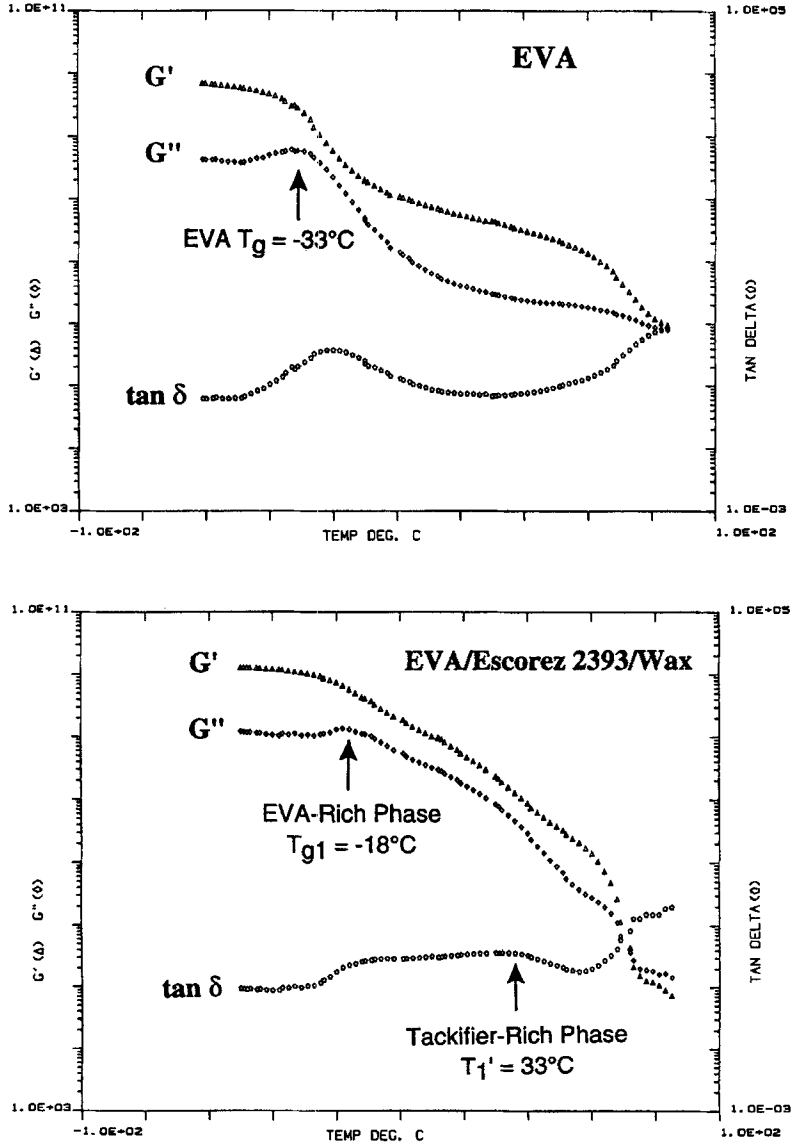

FIGURE 7 RDS-7700 loss modulus and loss tangent peak temperatures (frequency = 10 rad/s) are consistent with DMTA and modulated DSC results.

TABLE III Transition Temperatures of EVA and EVA/Escorez 2393/Wax

	Method	T_g *or* T_{g_1},°C	T_1',°C
EVA	Modulated		
	DSC	−31	–
	RDS-7700	−33	–
	DMTA	−17	–
EVA/Escorez	Modulated		
2393/Wax	DSC	−21	16
	RDS-7700	−18	33
	DMTA	−8	35

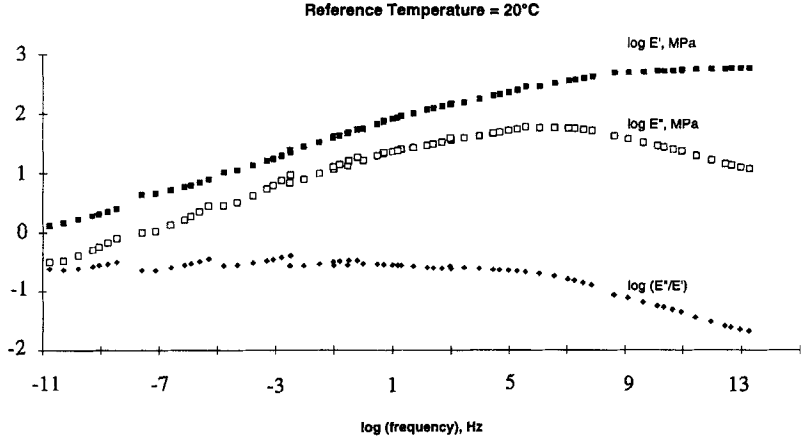

FIGURE 8 DMTA experiments show that the semi-crystalline structure of the HMA prevents rate-temperature superposition of its dynamic moduli (reference temperature = 20°C).

this behavior is explained using the viscoelastic properties of the EVA/Escorez 2393/Wax HMA.

From DMTA measurements, loss tangents as a function of frequency are shown in Figure 11. If the following equation, where v = Instron cross-head speed in the T-peel measurements and t_a = adhesive thickness = 0.43 mm [2]:

$$f = v/2t_a$$

is used calculate the T-peel debonding frequency, f, then the peel rates of 8.33×10^{-5}, 8.33×10^{-4} and 8.33×10^{-3} m/s correspond to the

TABLE IV Peel Analysis of EVA/Escorez 2393/Wax

Peel rate (m/sec)	*Temp °C*	*Failure Mode*	*%I*	*%C*	*Peel Force (Avg) N*	*Force (arrest)*	*Force (init.)*	*Distance Slip (cm)*	*Distance Stick (cm)*
8.33×10^{-5}	50	I	100	-	0.466	-	-	-	-
1.66×10^{-4}	50	I	100	-	0.809	-	-	-	-
8.33×10^{-4}	50	I	100	-	13.238	-	-	-	-
1.66×10^{-3}	50	C-I	35	65	24.565	-	-	-	-
3.33×10^{-3}	50	I-C	85	15	21.086	-	-	-	-
8.33×10^{-3}	50	C	-	100	36.038	-	-	-	-
8.33×10^{-5}	40	I	100	-	2.305	-	-	-	-
1.66×10^{-4}	40	I	100	-	2.236	-	-	-	-
8.33×10^{-4}	40	I	100	-	17.436	-	-	-	-
1.66×10^{-3}	40	I	100	-	21.555	-	-	-	-
3.33×10^{-3}	40	I	100	-	27.213	-	-	-	-
8.33×10^{-3}	40	I-C	70	30	30.596	-	-	-	-
8.33×10^{-5}	35	I	100	-	4.726	-	-	-	-
1.66×10^{-4}	35	I	100	-	10.199	-	-	-	-
8.33×10^{-4}	35	I	100	-	23.829	-	-	-	-
1.66×10^{-3}	35	I	100	-	24.447	-	-	-	-
3.33×10^{-3}	35	I	100	-	25.703	-	-	-	-
8.33×10^{-3}	35	I	100	-	29.135	-	-	-	-
8.33×10^{-5}	20	S-S	100	-	3.926	3.298	4.762	0.362	0.087
1.66×10^{-4}	20	S-S	100	-	3.403	0.948	5.858	0.345	0.075
8.33×10^{-4}	20	S-S	100	-	1.554	0.799	2.308	0.565	0.056
1.66×10^{-3}	20	S-S	100	-	1.649	0.785	2.515	0.735	0.080
3.33×10^{-3}	20	S-S	100	-	1.444	0.796	2.090	0.704	0.061
8.33×10^{-3}	20	S-S	100	-	1.231	0.732	1.730	0.623	0.133
8.33×10^{-5}	10	S-S	100	-	1.105	0.717	1.494	0.450	0.112
1.66×10^{-4}	10	S-S	100	-	1.007	0.760	1.255	0.350	0.102
8.33×10^{-4}	10	(S-S) I	100	-	0.672	0.448	0.891	0.904	0.127
1.66×10^{-3}	10	I	100	-	0.924	-	-	-	-
3.33×10^{-3}	10	I	100	-	0.549	-	-	-	-
8.33×10^{-3}	10	I	100	-	0.775	-	-	-	-
8.33×10^{-5}	0	S-S	100	-	0.691	0.580	0.797	0.350	0.087
1.66×10^{-4}	0	S-S	100	-	0.762	0.540	0.985	0.739	0.112
8.33×10^{-4}	0	S-S	100	-	0.765	0.562	0.964	0.710	0.097
1.66×10^{-3}	0	I	100	-	0.539	-	-	-	-
3.33×10^{-3}	0	I	100	-	0.559	-	-	-	-
8.33×10^{-3}	0	I	100	-	0.579	-	-	-	-

Failure Mode:
I = Interfacial Failure
C = Cohesive Failure in Adhesive
I-C = I > C
C-I = C > I
S-S = Stick-Slip

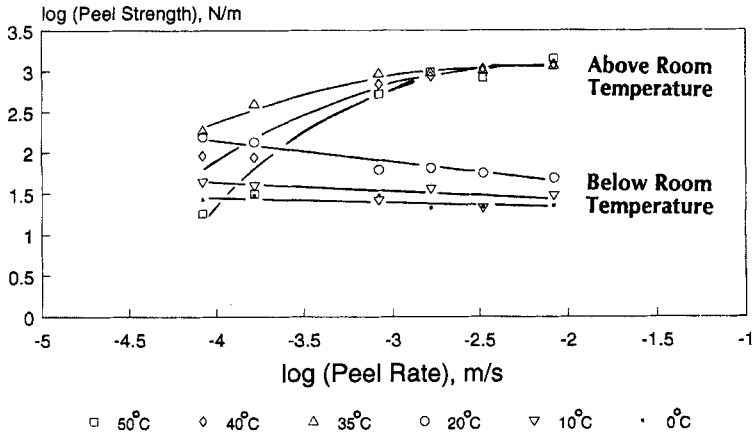

FIGURE 9 Peel strengths of the EVA/Escorez 2393/Wax model HMA to polypropylene depend on rate and temperature.

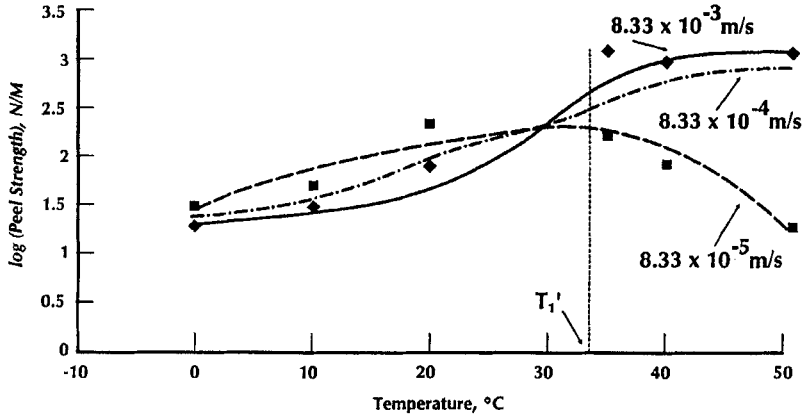

FIGURE 10 Peel behavior of EVA/Escorez 2393/Wax differs below and above T_1', the transition temperature of the HMA tackifier-rich phase.

debonding frequencies of 0.1, 1 and 10 Hz, respectively. These debonding frequencies are within the frequency range shown in Figure 11. It is noted that, at different test temperatures, the dependence of loss tangent of the bulk adhesive on frequency (Fig. 11) shows some resemblance to the dependence of peel strength on peel rate (Fig. 9). This is consistent with a previous result [2] that the HMA debonding term, D,

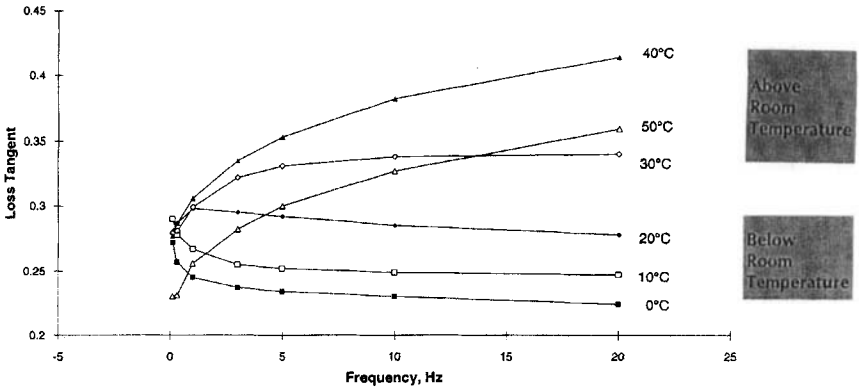

FIGURE 11 The DMTA loss tangent *versus* frequency behavior of EVA/Escorez 2393/Wax resembles to the peel strength *versus* peel rate behavior.

increases with the loss tangent of a HMA at the T-peel debonding frequency.

An attempt to shift the data in Figure 9 horizontally to form a master curve was not successful. This semi-crystalline adhesive does not obey the WLF rate-temperature equivalence. The reason for this is that the EVA is not amorphous, but rather has, based on the DSC experiment shown in Figure 4, $\sim$16 wt.% crystallinity. Also, according to Figure 7, T_{g_1} and T_1' of this adhesive are -18 and 33°C, respectively. Therefore, test temperatures were not well above the $T_g's$ of the adhesive, usually a requirement for horizontal shifting of viscoelastic data.

Failure Behavior of HMA

As detailed in Table IV, three distant regions of failure of the HMA are observed during peeling:

a. Interfacial Failure (I): The failure is at the interface of the adhesive layer and the PP film by visual inspection.
b. Cohesive Failure (C): Failure is within the bulk of the adhesive itself. After joint rupture, adhesive material is still attached to the inner sides of both PP films laminated by the HMA.

c. Stick-Slip Failure (S-S): A jerky peel is seen in which the observed peel force oscillates between rather well-defined limits. An autographic recording obtained in this region is shown in Figure 12. Attenuated total reflectance (ATR) spectra of the adhesive layer, the peeled PP film and the fresh PP film are shown in Figure 13. These spectra show that there is no difference between the fresh PP film and the peeled film. This suggests that stick-slip failure occurs with interfacial failure, as reported in Table IV. Also, the stick distance is always less than the slip distance as shown in Table IV and the drawing in Figure 12.

The cause of stick-slip failure is still not clear. In this kind of bond rupture, fracture occurs rapidly when the peel force reaches a maximum value – as the crack propagates at a speed faster than the testing speed. When stored energy is completely consumed, crack propagation stops, and the peel force reaches a minimum. As the peel force increases again to a maximum, another failure cycle occurs. Stick-slip phenomena also have been observed in tear [7], cleavage [8] and blister rupture [9].

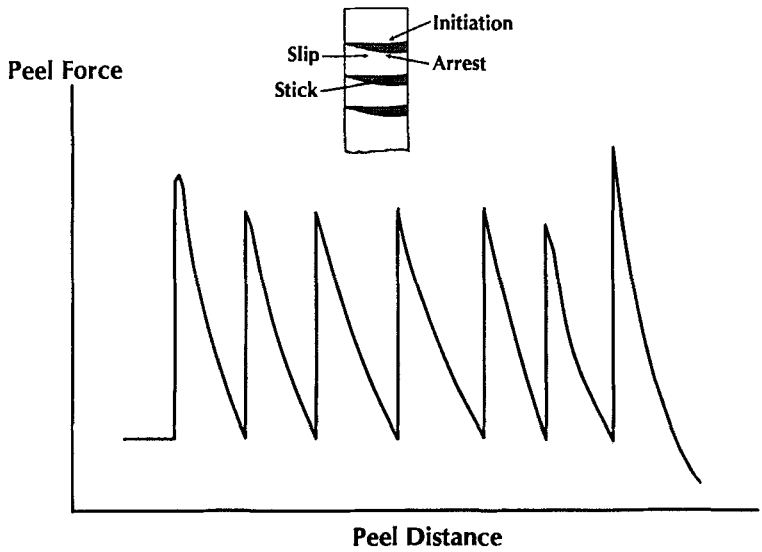

FIGURE 12 When stick-slip failure occurs, there are alternate rough and smooth regions on the peeled surface. Also, the rising and falling parts of the force trace correspond to the rough and smooth separations, respectively.

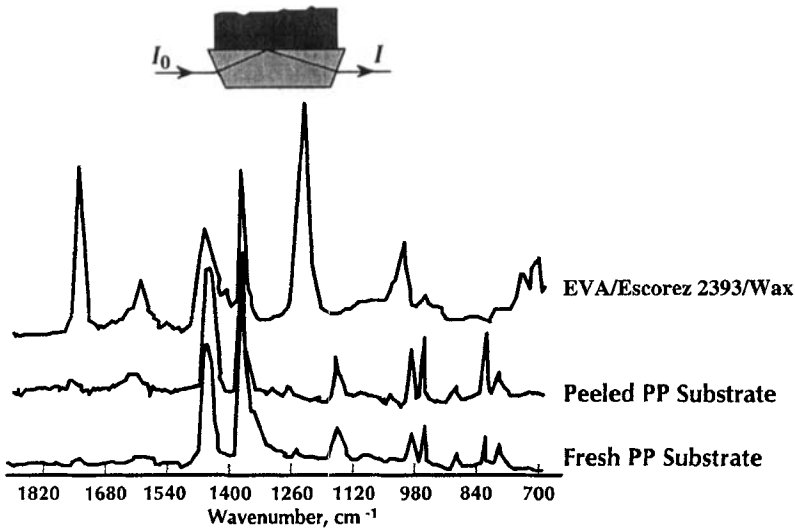

FIGURE 13 ATR spectra show no difference in the peeled PP and the fresh PP surfaces.

There are conflicting results in the literature concerning stick-slip failure. Gordon [10] observed that decreasing surface interactions will change stick-slip failure to continuous failure for a carboxylated adhesive. On the other hand, the opposite with a HMA has been found [2]. A higher bonding temperature, which causes increased surface interactions between a HMA and the PP substrate, changes stick-slip failure to continuous failure. In another example [10], roughening a substrate surface changed stick-slip failure to continuous failure with an acrylic adhesive bonded to cellophane. On the other hand, the opposite effect has been observed for EVA bonded to a rough and a smooth steel surface [11].

Figures 14–16 show the three separated curves from Figure 10. At a peel rate of 8.33×10^{-5} m/s (Fig. 14), the peel strength passes through a maximum at a temperature close to the transition temperature of the HMA tackifier-rich phase, T_1', which is equal to 33°C according to Figure 7. Two types of failure occur, slip-stick at lower temperatures and interfacial at higher temperatures, again separated roughly by T_1'.

At a higher peel rate, 8.33×10^{-4} m/s (Fig. 15), the peel strength increases up to an approximate plateau as temperature increases. A

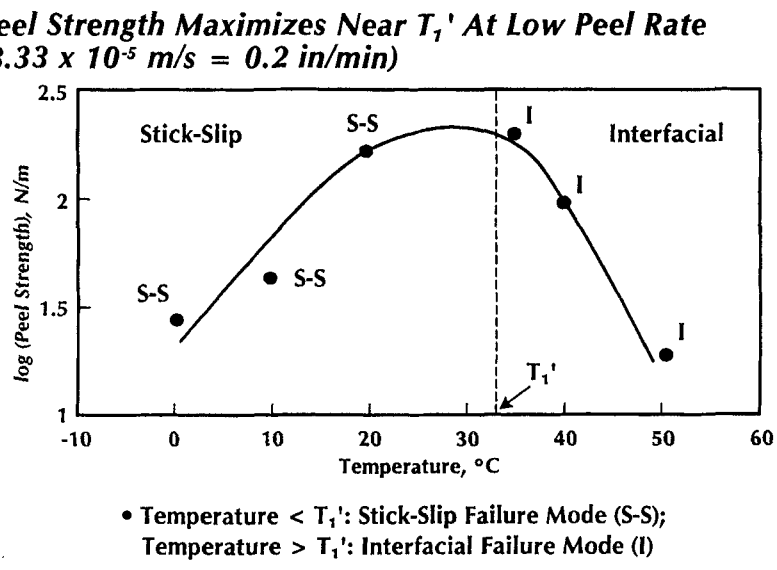

FIGURE 14 At a low peeling rate, the peel strength maximizes near T_1', accompanied by a change in failure mode.

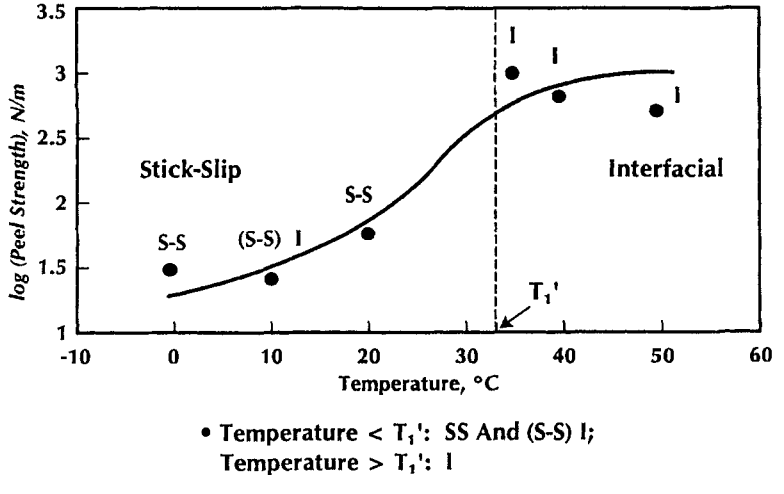

FIGURE 15 At an intermediate peeling rate, the peel strength increases up to an approximate plateau near T_1', accompanied by a change in failure mode.

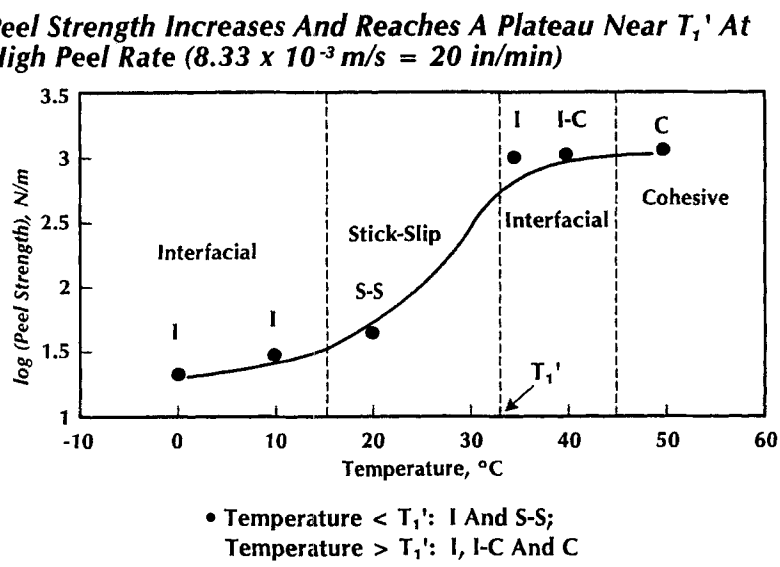

FIGURE 16 At a high peeling rate, the peel strength increases up to an approximate plateau near T_1'; multiple transitions in failure mode occur over the whole temperature range.

sharper rise is observed in the vicinity of T_1'. There is also a change in adhesive failure mode at a test temperature close to T_1' – stick-slip at lower temperatures and interfacial at higher temperatures.

At the highest peel rate, 8.33×10^{-3} m/s (Fig. 16), again, peel strength rises gradually with test temperature and a sharper rise occurs in the vicinity of T_1'. The bond fails interfacially in a continuous way at 0 and 10°C, but in a stick-slip mode at 20°C. At 35 and 40°C, failure is again at the interface, whereas, at the highest temperature of 50°C, failure is cohesive. A more in-depth discussion of the failure behavior of the HMA in Figure 16 follows.

As discussed in the "Introduction" and the previous section, it has been established that the peel behavior of an adhesive joint depends strongly upon the bulk viscoelastic response of the adhesive. Overall, the adhesive behavior in Figure 16 can be related to the viscoelastic response of the adhesive. Near the glass-like state, interfacial failure occurs. As temperature decreases, the cohesive strength of the adhesive increases and, at a certain temperature, exceeds the interfacial strength. In this case, the interface is the path of least resistance to

rupture. Stick-slip corresponds to a transition from glass-like to rubber-like behavior, where failure is again interfacial.

During interfacial failure at low test temperatures (0–10°C), a smooth adhesive surface is observed after peeling. This is due to the fact that the adhesive has a glass-like behavior at 0–10°C ($T_1' = 33$°C), hence there is clean interfacial failure with a smooth debonded adhesive surface. At slightly higher test temperatures ($\sim$ 15–33°C), where stick-slip occurs, there are alternate rough and smooth regions on the peeled surface. Also, the rising and falling parts of the force trace correspond with rough and smooth separations, respectively (Fig. 12). However, at still higher test temperatures ($\sim$ 35–45°C), a rough adhesive surface is observed. The roughness is associated with the formation of small voids on the surface and in the bulk of the adhesive. This is due to the fact that, at $\sim$ 35–45°C, the adhesive is in the rubbery state, where clean interfacial failure still occurs, but with a rough peeled adhesive surface. The roughness of the adhesive surface as well as the peel strength increase with increasing peel rate at these high temperatures. As shown in Figure 11, loss tangent of the HMA increases with frequency at 30–50°C. Therefore, one explanation for the observed HMA failure modes is that, in the rubbery state, much energy dissipation within the adhesive occurs. Similar to the behavior of the loss tangent with a change in frequency, this energy dissipation increases with increasing peel rate. The result is a rise in peel strength. Also, it is expected that, with an increase in the peel strength of an adhesive in the rubbery state, roughness on the peeled surface will increase. At still higher test temperatures (> 45°C), cohesive failure of the HMA will occur.

It is noted that, with increasing test temperature, the joint goes from a stick-slip to an interfacial mode at lower peel rates (Figs. 14–15 and Tab. IV), whereas it goes from an interfacial to a stick-slip mode at a higher peel rate (Fig. 16 and Tab. IV). An explanation for this observation is that, at lower peel rates, it may be necessary to peel the HMA from the PP at a lower temperature, even lower than 0°C, in order to observe interfacial failure. Of course, one forseeable complication is that the PP substrate can become glassy (T_g of the PP substrate is ~ -10°C) at lower test temperatures.

Also, it is noted that, at the highest test temperature (50°C), the joint fails interfacially at lower peel rates (Figs. 14–15 and Tab. IV),

whereas it fails cohesively at a higher peel rate (Fig. 16 and Tab. IV). An explanation for this observation is that, at 50°C, loss tangents at 0.1 and 1 Hz, which correspond to peel rates of 8.33×10^{-5} and 8.33×10^{-4} m/s, respectively, is small compared with the loss tangent at 10 Hz, which corresponds to a peel rate of 8.33×10^{-3} m/s (Fig. 11). The higher degree of energy dissipation in the HMA at this higher peel rate may cause the adhesive to fail cohesively. Of course, a further increase in test temperature approaching the HMA's T_m (68°C) moves the response into the viscous flow region. The polymeric adhesive will show more liquid-like behavior and has less mechanical strength, even lower than that of the interface. Therefore, failure still occurs within the bulk of the adhesive.

One final comment learned from Figures 14–16: to maximize HMA peel strength at ambient temperature, it is desired to formulate the EVA polymer (or other semi-crystalline polyolefin) with a compatible tackifier that yields a tackifier-rich phase with a transition temperature (T_1') in the vicinity of room temperature. As discussed before in Figure 5, when wax is eliminated from the EVA/Escorez 2393/Wax HMA, the peak tan δ in the EVA-rich phase is decreased, but that in the tackifier-rich phase is increased. At a temperature of 20°C and a peel rate of 8.33×10^{-4} m/s, the peel strength with the EVA/Escorez 2393/Wax HMA is 61 N/m, whereas that with the EVA/Escorez 2393 HMA is 180 N/m. Again, this indicates that the tackifier-rich phase plays a more important role in influencing the peel strength, as in the case of block copolymer/tackifier blends [3].

CONCLUSIONS

Conclusions are summarized below.

- Similar to block copolymer/tackifier blends [3], an ethylene-vinyl acetate copolymer (EVA)/tackifier/wax HMA blend has two phases, an EVA-rich and a tackifier-rich phase, in the amorphous region of this HMA.
- The T-peel adhesion between this model EVA adhesive and the untreated PP film is both rate and temperature dependent. However, the influence of rate and temperature on peel adhesion is not

equivalent, causing failure of rate-temperature superposition and multiple transitions in failure mode. One major failure locus transition occurs at T_1', the transition temperature of the HMA tackifier-rich phase.

- At different test temperatures, the dependence of the peel strength on peel rate shows some resemblance to the dependence of the loss tangent of the bulk adhesive on frequency. This is consistent with a previous result [2] that the HMA debonding term, D, varies with the loss tangent of a HMA at the T-peel debonding frequency.
- At low peel rates, the peel strength shows a maximum at a temperature that corresponds to the T_1' of the HMA. At high peel rates, the peel strength rises with increasing temperature, but reaches an apparent plateau at the temperature that again corresponds to the T_1' of the HMA.
- To optimize HMA peel strength at ambient temperature, it is desired to formulate an EVA polymer (or other semi-crystalline polyolefins) with a compatible tackifier that yields a tackifier-rich phase with a transition temperature (T_1') in the vicinity of room temperature.

Acknowledgments

The authors would like to thank Exxon Chemical Company for permission to publish this work.

References

[1] Gent, A. N. and Petrich, P. P., *Proc. R. Soc. London Ser.* **A 310**, 433 (1969).
[2] Tse, M. F., *J. Adhesion* **48**, 149 (1995).
[3] Tse, M. F., *J. Adhesion Sci. Technol.* **3**(7), 551 (1989).
[4] Ferry, J. D., *Viscoelastic Properties of Polymers* (John Wiley & Sons, New York, 1980), 3rd ed.
[5] Kaeble, D. H., *J. Colloid Sci.* **19**, 413 (1964).
[6] Bitner, J. L., Rushford, J. L., Rose, W. S., Houston, D. L. and Riew, C. K., *J. Adhesion* **13**, 3 (1981).
[7] Greensmith, H. W., *J. Polym. Sci.* **21**, 175 (1956).
[8] Bailey, A. L., *J. Appl. Phys.* **32**, 1407 (1961).
[9] Bikerman, J. J., in *Testing of Polymers*, **Vol. 4**, Brown, W. E., Ed. (Interscience, New York, 1969), pp. 213–235.
[10] Gardon, J. L., *J. Appl. Polym. Sci.* **7**, 625 (1963).
[11] Racich, J. L. and Koutsky, J. A., *J. Appl. Polym. Sci.* **19**, 1479 (1975).